DECORATION OF CARBON NANOTUBES
WITH CERIUM (IV) OXIDE

S.Ya. Brichka[1], I.B. Yanchuk[2]*, A.A. Konchits[2], S.P. Kolesnik[2], A.V. Yefanov[2], A.V. Brichka[1], N.T. Kartel[1]

[1]*Chuiko Institute of Surface Chemistry of National Academy of Sciences of Ukraine*
17 General Naumov Street, Kyiv 03164, Ukraine
[2]*Lashkarev Institute of Semiconductor Physics of National Academy of Sciences of Ukraine*
41 Nauky Ave., Kyiv 03028, Ukraine

Cerium (IV) oxide (ceria) nanoparticles, 6–10 nm in size, supported on carbon nanotubes (CNTs) were prepared by a chemical reaction between $Ce(NO_3)_3$ and NaOH. The effective processing parameters of ceria particles size were discussed. $CNTs/CeO_2$ hybrids were characterized by transmission electron microscopy (TEM), selected area electron diffraction (SAED), Raman and electron paramagnetic resonance (EPR) spectroscopy. SAED and Raman spectroscopy showed that the CeO_2 particles had a cubic crystal structure. EMR spectroscopy showed two paramagnetic signals related to CNTs and a third one belonging to paramagnetic defects of CeO_2.

INTRODUCTION

Chemical modification of carbon nanotubes leads to changes in their physical and chemical properties [1, 2]. Recent studies on corrosion behavior of Zn deposits containing nanoparticles reported that the content of CNTs in the deposits improved the corrosion resistance as compared to zinc coating. In many cases the CNTs act as physical barrier to the corrosion process by filling in crevices, gaps, and micro holes on the surface of deposit [3]. The results [4] showed that addition of CNTs to the deposition process of nickel significantly increased its resistance to corrosion. The improvement in corrosion resistance is due to the CNTs acting as physical barriers to corrosion process by filling in crevices, gaps and micron holes on the surface of nickel coating. Another reason is that CNTs evenly distributed in the nickel coating increase corrosion potential of the composite coating towards more positive values restricting localized corrosion and result in more homogenous corrosion.

Replacement of extremely toxic anticorrosive pigments (chromates, vanadates and nitrates) in ecologically friendly analogues is a major chemical problem [5]. Cerium compounds show satisfactory results in the protection of iron, aluminium and other metals from corrosion [6, 7]. There are also other spheres where cerium oxide is used. Cerium oxide is a catalyst in the oxidation of CO and NO that is important for cleaning exhaust gases and in other technological processes [8, 9]. The catalytic activity of ceria for H_2 and CO production from fuels is described in [10]. Cerium oxides are used in fuel cells as solid state conductors [11]. Ceria adsorbents are used for the removal of toxic Cr (VI) from water with an adsorption capacity of 30.2 mg·g^{-1} and in medicine [12, 13]. The use of ceria to sense molecular oxygen has been investigated [14]. Ceria is a good polishing material which has been used commercially [15]. Cerium oxide powders are often used as fillers in polymers and in ceramics [16, 17].

Combining the effect of CNTs and cerium oxide is expected to produce highly efficient environmentally friendly anti-corrosion pigments. The purpose of our work is the synthesis of CNT/CeO_2 hybrids and testing them as anticorrosive pigments.

EXPERIMENTAL

Sample preparation. Certificated catalytic multiwalled carbon nanotubes (CNTs, Nanothinx S.A.) having a diameter of 12–31 nm, 15–35 walls and 97% purity (about 2% is iron catalyst and less 1% is pyrolytic carbon) were used. CNTs were modified by the following reaction

$$4Ce(NO_3)_3 + 12NaOH + O_2^{air} = 4CeO_2 + 12NaNO_3 + 6H_2O.$$
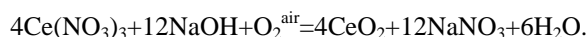
6.25 g of CNTs was placed in about 15 ml of distilled water. Then 4 ml 0.5M (16.3 ml 1M)

* corresponding author *yanchuk@isp.kiev.ua*

_____

$Ce(NO_3)_3$ solution was added. Under mixing 6 ml 1M (24.5 ml 2M) NaOH solution was added until the pH was 8–9. The solid was filtered, rinsed and dried at 383 K. Two samples of $CNTs/CeO_2$ (5.2%) and $CNTs/CeO_2$ (31%) with different content of ceria were prepared.

Corrosion testing. The anticorrosion properties of $CNTs/CeO_2$ pigments were tested in an amine covering. Dispersed pigment covering was placed on a panel of 2024-T3 aluminium scavenged by a standard four bath clearing process and scribed at widths of approximately 2 mm. Corrosion tests of the panels were carried out in freely aerated 3.5% NaCl solution for 3000 h together with $SrCrO_4$ reference pigment. After the test, the bottom halves of the panels were stripped for visual inspection.

Samples characterization. The carbon nanotubes were identified by transmission electronic microscope (JEM-100CXII). A crystalline structure of samples was verified by the selected area electron diffraction pattern. The Raman spectra were detected using a double monochromator, a cooled photomultiplier employing standard photon counting technique, and DPSS laser at 532 nm for excitation. Estimated accuracy of determining the peak position was of 1 cm^{-1}. Electron magnetic resonance measurements were carried out at the temperature range of 35–300 K using X-band (microwave frequency ν=9.5 GHz) electron paramagnetic resonance spectrometer (Radiopan X-2244) with 100 kHz modulation of magnetic field. Estimated accuracy of the determining the g-factor was of $\pm 5 \times 10^{-4}$ and $\pm 3 \times 10^{-2}$ approximately for the narrow and broad lines, respectively. The relative accuracy of EMR intensity measurements was of ±30%.

RESULTS AND DISCUSSION

Formation of ceria. The ultrafine CeO_2 powders were synthesized by using flash combustion, mechanochemical processing, co-precipitation, homogeneous precipitation, electrochemical synthesis, hydrothermal, and solvothermal processes. Recently a significant advancement has been made in developing environmentally friendly and economically efficient ways of producing controlled ceria nanostructures via aqueous-phase synthesis method. Polyhedra, rods, wire, cubes, sphere, tadpole-shaped wire, triangular plate, and hollow structure, nanotube-like structure of CeO_2 are selectively obtained by

changing conditions [18]. Often synthesis of nanosized CeO_2 carry out the alcohol aqueous environment. We have chosen exclusively the neutral aqueous-phase synthesis method in order to make the scaling easy.

Photos of electronic images of CNTs are presented in Fig. 1 which displays the characteristics of CNTs described in the experimental part.
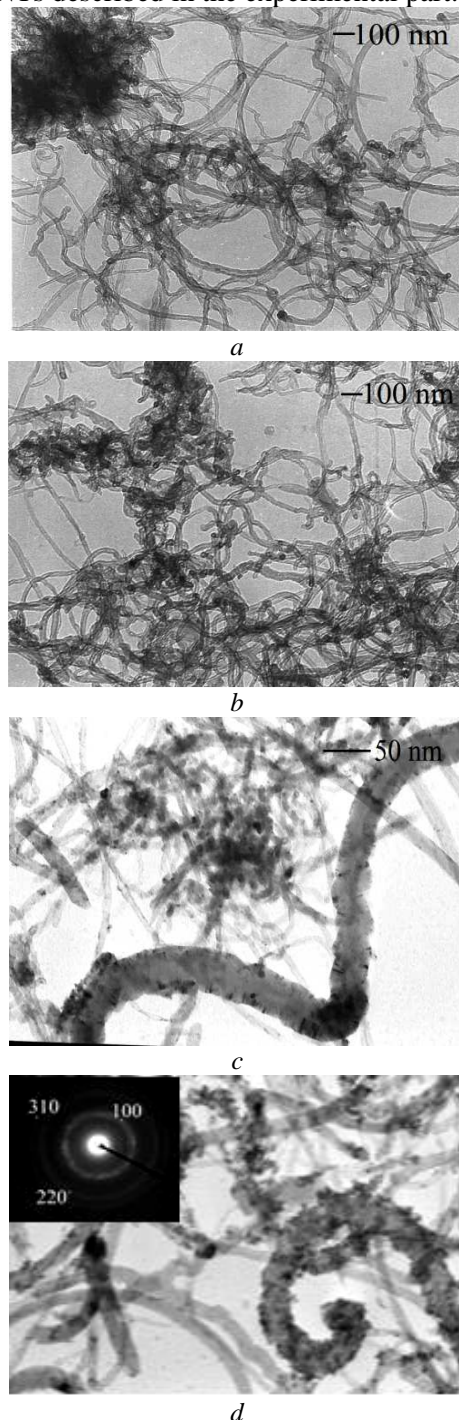

Fig. 1. TEM images of initial CNTs (*a,b*), and CNTs modified by ceria of 5.2% (*c*) and 31% mass. (*d*)

The photos show that nanotubes form conglomerates. The electronic images (Fig. 1c,d) of modified CNTs testify to particles which decorate them. SAED indicates the rings pattern of nanoparticles that can be indexed using the face-centered cubic polycrystalline structure of CeO_2. Diffusiveness signals of weak crystallization and influence of dimensional effect. The size of 6–10 nm particles fluctuates in a range according to TEM.

Raman spectroscopy of carbon nanotubes. A spectrum of initial CNTs (Fig. 2a,1) consists of two clear separate bands – D 1352 cm^{-1} and G 1579 cm^{-1} with the intensity ratio $I_D/I_G = 0.38$.
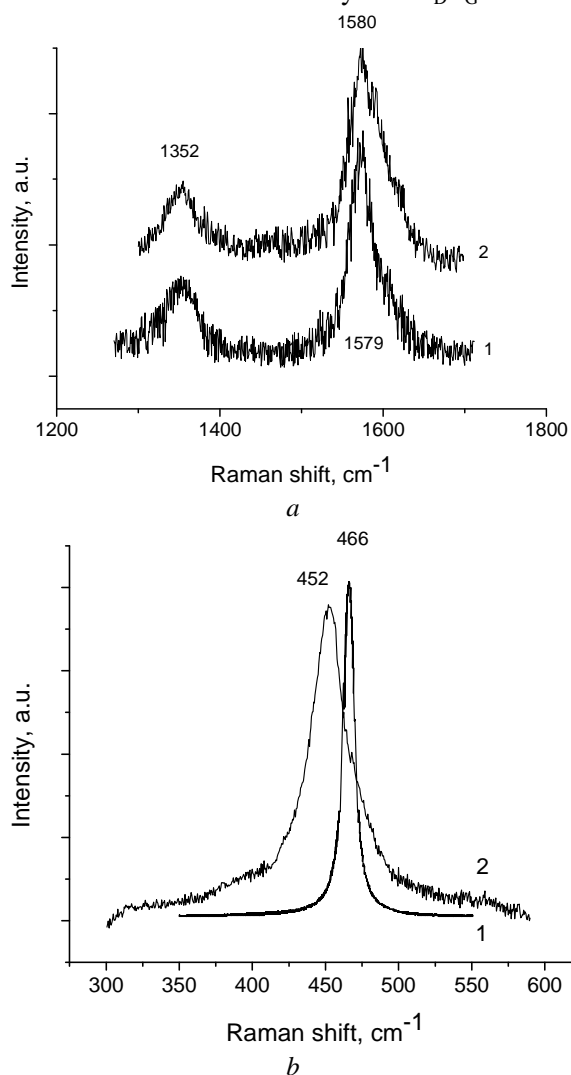

a

b

Fig. 2. Raman spectra of CNTs (*1*), CNTs modified by ceria of 31% mass. (*2*) in "carbon" region (*a*); ceria single crystal (*1*) and CNTs modified by ceria of 31% mass. (*2*) in "ceria" region (*b*)

The G peak is usually assigned to zone centre phonons of E_{2g} symmetry and the D peak, which is the breathing mode of A_{1g} symmetry, involves

phonons near the K zone boundary of sp^2-hybridizing carbon. After depositions of ceria, a spectrum of modified CNTs (Fig. 2a,2) has D-band 1352 cm^{-1} and G-band 1580 cm^{-1} with the $I_D/I_G = 0.26$.

The Raman spectra for CNTs synthesized by matrix method have bands at 1302 and 1590 cm^{-1} that for disordered graphite are located in the range of 1300–1350 and 1570–1585 cm^{-1} [19]. The increasing width of G-peak from 37 to 46 cm^{-1} for modified CNTs leads to the decreasing in I_D/I_G. As G-peak broadening is detected, the bond-angle distortion at the carbon atom in six fold aromatic rings can be explained by the influence of synthetic procedure and ceria interaction with carbon surface of the nanotubes.

CNTs decorated with 31% CeO_2 show clear Raman signal in the "ceria region". It was impossible to detect the ceria signal of CNTs with 5.2% mass. CeO_2 due to small amount of ceria clusters and their high dispersion. Raman spectra have shown a strong peak at 452 cm^{-1} with full width at half maximum (Γ) of 26.5 cm^{-1} (Fig. 2b,2). The peak is related to F_{2g} mode of CeO_2 fluorite structure what corresponds to SAED data. The Raman peak of CeO_2 single crystal is much narrower ($\Gamma=13.5$ cm^{-1}) and has much higher peak position at 466 cm^{-1} (Fig. 2b,1). A significant downshift of 14 cm^{-1} and broadening of 13 cm^{-1} of F_{2g} mode as compared to the bulk ceria indicate the presence of nanosized crystals [20, 21]. We used a correlations $\Gamma = 10 + 124.7/d_g$ between Γ and grain size d_g for estimation of ceria nanocrystal size. The data on the size of CeO_2 particles obtained from TEM and Raman spectroscopy ($d_g = 7.6$ nm) correlate. The main reason for broadening of F_{2g} mode is disorder in the oxygen sublattice resulting grain size-induced non-stoichiometry. Therefore, we estimated the defect concentration to be about 8×10^{20} cm^{-3}.

Influence of synthesis conditions on ceria particles size. By means of synthesis of CeO_2 from $CeCl_3$ at 283 K the particles of about 6 nm are obtained on oxidized carbon nanotubes through a stage of heating at 723 K. What precipitating cerium hydroxide in more alkaline solution or carrying out the reaction at 293 K, the average size of particles increases to 10–15 nm [22]. By a similar technique CeO_2 nanoparticles in the size of 3–8 nm are synthesized being placed on two-layer carbon nanotubes [23]. CeO_2 with average grain size of 4 nm was synthesized

from $Ce(NO)_3$ and $NaOH$ in alcohol aqueous solution ($V_{alcohol}:V_{water}=1:1$) with high-intensity ultrasonic radiation at room temperature [24].

We synthesized the cerium oxide particles of 6–10 nm corresponding to those described in scientific works. It should be point out that the non-templating synthesis reduces the cost of CeO_2. When using special additives, ultrasonic processing and other expensive approaches [18], it is possible to make the size of particles one-half of initial one.

Authors of [22] have come out with the assumption that oxygen chemisorbed atoms on CNTs are the formation centers of oxide nanoparticles. It is obvious that uniformity of CNT decoration [23, 24] contradicts the nature of their surface. When carbon oxidation of nanotubes occurs, first of all a reaction proceeds with participation of graphene defects (the ends of nanotubes and non-integral sites of their surface) that would lead to selectivity of the centers of CeO_2 adsorption. In our opinion, one of the formation reasons of nanosized ceria is templating action of CNTs substrate. Nanotubes have nanosized, closed surface, with high degree of curvature and with set of heterogeneous contacts. These properties really can favorably influence on the formation of small oxide particles.

EPR spectroscopy of carbon nanotubes. Intensive and broad $\Delta H_{pp} \approx 1.5$ kG EPR signals with $g \approx 2.15$ caused by the presence of residual iron catalytic nanoparticles are observed in of samples both CNTs and modified CNTs (Fig. 3).
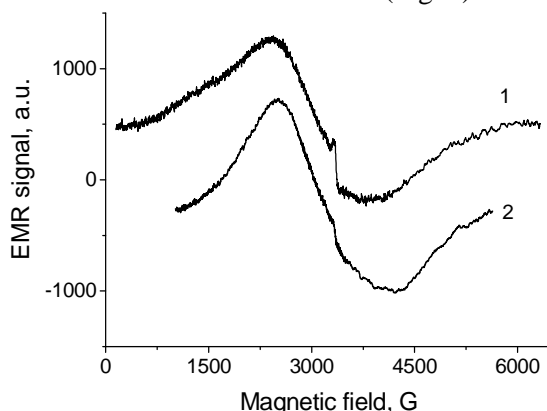

Fig. 3. EPR spectra of CNTs (*1*) and those modified by ceria of 31% mass. (*2*) at 300 K

Narrower EMR lines $\Delta H_{pp} \approx 70$ G of smaller intensity caused by the presence of carbon-related defects are also observed in the samples (Fig. 3, spectra central part). The value of g-factor for these defects (2.003) is typical of the carbon dan-

gling bonds. We will disregard the influence of metal catalysts on EPR signal but focus on carbon-related ones.

In order to obtain more information about the carbon-related defects, we studied their behavior depending on the temperature (Fig. 4).
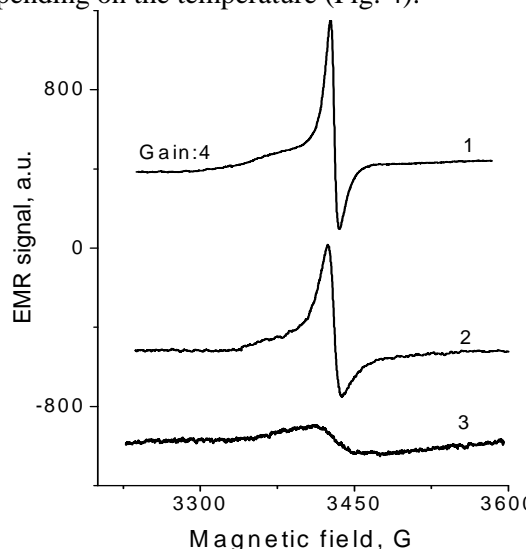

Fig. 4. EPR spectra of CNTs at 25 (*1*), 70 (*2*) and 300 K (*3*)

At low temperatures the shape of the carbon related EPR line is complicated. It can be describe as a sum of two broad $\Delta H_{pp} \approx 50$ G and narrow $\Delta H_{pp} \approx 7$ G contributions to the profile width at 25 K (Fig. 4, *1*). The broad part does not change roughly the line width within the 25 to 300 K temperature range. The line width of narrow part increases gradually due to elevation of spin relaxation processes at high temperatures.

The line widths of both contributions are equal at room temperature and form a single contour of EPR absorption with a Lorentz line shape (Fig. 4, 3).

The EPR integral intensity follows the Curie law ($I \sim C/T$) between 25 and 100 K specifying the mainly localized character of the paramagnetic centers. A visible growth of I (T) is sharply slowed down at T < 25 K what is caused partly by the saturation effects due to sudden decreasing of the spin relaxation rate below 20 K [25].

We believe that a principal cause of the EPR spectrum modification is the interaction of the paramagnetic subsystem of free carriers with the localized defects (carbon dangling bonds) in the nanotubes structure [26]. In this model, the EPR line width is formed by the interaction between subsystems and grows gradually as the temperature increases due to spin relaxation contribution

of free carriers [27]. From the described point of view the presence of broad part to EPR contribution at low T (Fig. 4, *1*) indicated the existence of an additional broadening mechanism due to either an interaction with other impurities [28] or different acting to the inner and outer nanotube sides [25]. The exchange coupling model also forecasts the Pauli contribution in the paramagnetic susceptibility at high T and the Curie law at low T.

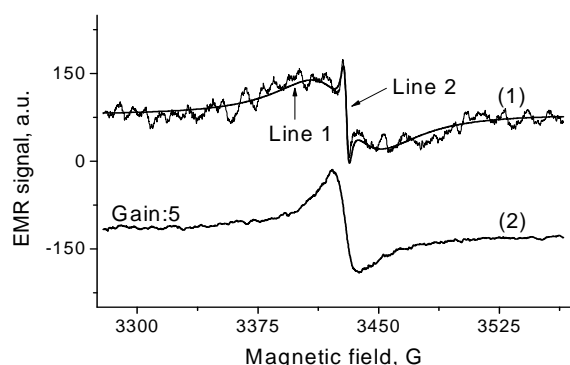In the modified CNTs system one more EPR signal with close g-value 2.0028 is observed at room temperature (Fig. 5, *2*).

Fig. 5. EPR spectra of CNTs modified by ceria of 31% mass. at 300 (*1*) and 70 K (*2*)

The line width of the signal depends on the oxygen atmosphere content so values of $\Delta H_{pp} = 4$, 5 and 8 G change in evacuation. The signal belongs to defects of CeO_2 structure [29]. It is not possible to track down the temperature behavior of this signal because it masks more intensive EPR signal (line *1*) of the nanotubes (Fig. 4). A total concentration of the paramagnetic centers for the modified sample is $N_s \approx 10^{20}$ cm^{-3}.

Anticorrosion properties of modified carbon nanotubes. Panels containing chromate, CNTs/CeO$_2$ (5.2%) and CNTs/CeO$_2$ (31%) primers were used for the corrosion test. Damage protection is demonstrated by results of corrosion exposure of scribed samples are shown by all primers. After 3000 h in salt spray chamber of chromate panel, the scribe on the panel remained shiny with no visible sign of corrosion. The CNTs/CeO$_2$ (5.2%) panel did not show significant signs of corrosion on the scribe but it was not as shiny as that of the chromate panel. The CNTs/CeO$_2$ (31%) panels showed visual indication of corrosion at 18%. We think that the speed of ceria oxide releasing on metal surface plays a critical role in the anticorrosion effect. Additional studies will be done to understand the anticorrosion properties of the pigments. These results in-

dicate a reasonable corrosion inhibition for CNTs/CeO$_2$ specimens.

CONCLUSIONS

The ceria nanoparticles supported on carbon nanotubes about 6–10 nm were synthesized by chemical reaction between Ce(NO$_3$)$_3$ and NaOH. The synthesis was realized in aqueous solution at room temperature that reduces the cost of the preparation procedure of nanosized ceria. EPR spectroscopy showed two paramagnetic signals of CNTs and the third one belonging to paramagnetic defects of CeO$_2$. The CNTs/CeO$_2$ (5.2%) could be used as a substrate preparation component to replace the currently utilized chromate containing surface treatments and provide the basis for long lasting coating system for aluminium alloys.

ACKNOWLEDGEMENTS

REFERENCES

1. *Brichka S.Ya., Prikhod'ko G.P., Brichka A.V., Kislii Yu.A.* Synthesis of bimodified carbon nanotubes – a nanocomposite material // Inorg. Mater. – 2004. – V. 40, N 12. – P. 1276–1279.

2. *Brichka S.Ya., Prikhod'ko G.P., Brichka A.V. et al.* Physicochemical properties of multilayer N-containing carbon nanotubes // Russ. J. Phys. Chem. – 2004. – V. 78, N 1. – P. 121–125.

3. *Chen X.H., Chen C.S., Xiao H.N. et al.* Corrosion behavior of carbon nanotubes–Ni composite coating // Surf. Coat. Technol. – 2005. – V. 191, N 2–3. – P. 351–356.

4. *Praveen B.M., Venkatesha T.V., Arthoba Naik Y., Prashantha K.* Corrosion studies of carbon nanotubes–Zn composite coating // Surf. Coat. Technol. – 2007. – V. 201, N 12. – P. 5836–5842.

5. *Amirudin A., Thierry D.* Evaluation of anticorrosive pigments by pigment extract studies, atmospheric exposure and electrochemical impedance spectroscopy // Prog. Org. Coat. – 1995. – V. 25, N 4. – P. 339–355.

6. *Phani A.R., Gammel F.J., Hack T., Haefke H.* Enhanced corrosion resistance by sol-gel-based ZrO$_2$-CeO$_2$ coatings on magnesium alloys // Mater. Corros. – 2005. – V. 56, N 2. – P. 77–82.

7. *Liu W., Cao F., Chang L. et al.* Effect of rare earth element Ce and La on corrosion behaviour of AM60 magnesium alloy // Corros. Sci. – 2009. – V. 51, N 6. – P. 1334–1343.

8. *Marban G.I., Valdes-Solıs T.* Preferential oxidation of CO by CuO_x/CeO_2 nanocatalysts prepared by SACOP. Mechanisms of deactivation under the reactant stream // Appl. Catal. A. – 2009. – V. 361, N 1–2. – P. 160–169.

9. *Roy S., Hegde M.S., Madras G.* Catalysis for NO_x abatement // Appl. Energy. – 2009. – V. 86, N 11. – P. 2283–2297.

10. *Hirata Y., Terasawa Y., Matsunaga N., Sameshima S.* Development of electrochemical cell with layered composite of the Gd-doped ceria/electronic conductor system for generation of H_2–CO fuel through oxidation–reduction of CH_4–CO_2 mixed gases // Ceram. Int. – 2009. – V. 35, N 5. – P. 2023–2028.

11. *Steele B.C.H.* Fuel-cell technology: Running on natural gas // Nature. – 1989. – V. 400. – P. 619–621.

12. *Di Z., Ding J., Li Y. et al.* Chromium adsorption by aligned carbon nanotubes supported ceria nanoparticles // Chemosphere. – 2006. – V. 62, N 5. – P. 861–865.

13. *Colon J., Herrera L., Smith J. et al.* Protection from radiation-induced pneumonitis using cerium oxide nanoparticles // Nanomed. Nanotechnol. Biol. Med. – 2009. – V. 5, N 2. – P. 225–231.

14. *Ghom S.A., Zamani C., Nazarpour S. et al.* Oxygen sensing with mesoporous ceria–zirconia solid solutions // Sens. Actuators. B.– 2009. – V. 140, N 1. – P. 216–221.

15. *Wang L., Zhang K., Song Zh., Feng S.* Ceria concentration effect on chemical mechanical polishing of optical glass // Appl. Surf. Sci. – 2007. – V. 253, N 11. – P. 4951–4954.

16. *Armini S., De Messemaeker J., Whelan C.M, et al.* Composite polymer core–ceria shell abrasive particles during oxide CMP: A defectivity study // J. Electrochem. Soc. – 2008. – V. 155, N 9. – P. 653–660.

17. *Park H.J., Kwak C., Lee K.H. et al.* Interfacial protonic conduction in ceramics // J. Eur. Ceram. Soc. – 2009. – V. 29, N . – P. 2429–2437.

18. *Yuan Q., Duan H., Li L. et al.* Controlled synthesis and assembly of ceria-based nanomate-rials // J. Colloid Interface Sci. – 2009. – V. 335, N 2. – P. 151–167.

19. *Yanchuk I.B., Koval's'ka E.O., Brichka A.V., Brichka S.Ya.* Raman scattering studies of the influence of thermal treatment of multi-walled carbon nanotubes on their structural characteristics // Ukr. J. Phys. – 2009. – V. 54, N 4. – P. 407–412.

20. *Weber W.H., Hass K.C., McBride J.R.* Raman study of CeO_2: second-order scattering, lattice dynamics, and particle-size effects // Phys. Rev. B. – 1993. – V. 48, N 1. – P. 178–185.

21. *Kosacki I., Suzuki T., Anderson H.U., Colomban Ph.* Raman scattering and lattice defects in nanocrystalline CeO_2 thin films // Solid State Ionics. – 2002. – V. 149, N 1–2. – P. 99–105.

22. *Li Y., Ding J., Chen J. et al.* Preparation of ceria nanoparticles supported on carbon nanotubes // Mater. Res. Bull. – 2002. – V. 37, N 2. – P. 313–318.

23. *Wei J., Ding J., Wu D. et al.* Coated double-walled carbon nanotubes with ceria nanoparticles // Mater. Lett. – 2005. – V. 59. – P. 322–325.

24. *Zhang D., Shi L., Fu H., Fang J.* Ultrasonic-assisted preparation of carbon nanotube/cerium oxide composites // Carbon. – 2006. – V. 44, N 13. – P. 2849–2867.

25. *Nafradi B., Nemes N.M., Feher T. et al.* Electron spin resonance of single-walled carbon nanotubes and related structures // Phys. Status Solidi. B. – 2006. – V. 243, N 13. – P. 3106–3110.

26. *Beuneu F., l'Huillier C., Salvetat J.P. et al.* Modification of multiwall carbon nanotubes by electron irradiation: An ESR study // Phys. Rev. B. – 1999. – V. 59. – P. 5945–5952.

27. *Fabian J., Das Sarma S.* Phonon-Induced Spin Relaxation of Conduction Electrons in Aluminum // Phys. Rev. Lett. – 1999. – V. 83. – P. 1211–1214.

28. *Salvetat J.P., Feher T., L'Huillier C. et al.* Electron spin resonance in alkali doped SWCNTs // Phys. Rev. B. – 2005. – V. 72. – P. 7544–7549.

29. *Trovarelli A.* Catalysis by ceria and related materials. – London: Imperial College Press, 2002. – 528 p.

_____

Декорування вуглецевих нанотрубок оксидом церію (IV)

**С.Я. Бричка, І.Б. Янчук,
А.А. Кончиць, С.П. Колесник, А.В. Єфанов,
А.В. Бричка, М.Т. Картель**

*Інститут хімії поверхні ім. О.О. Чуйка Національної академії наук України
вул. Генерала Наумова 17, Київ 03164, Україна
Інститут фізики напівпровідників ім. В.Є. Лашкарьова Національної академії наук України
пр. Науки 41, Київ 03028, Україна, yanchuk@isp.kiev.ua*

Наночастинки оксиду церію (IV) розміром 6-10 нм одержано на вуглецевих нанотрубках (ВНТ) за хімічною реакцією між $Ce(NO_3)_3$ і $NaOH$. Встановлено ефективні параметри синтезу наночастинок оксиду церію. Нанокомпозити $ВНТ/CeO_2$ охарактеризовано за допомогою трансмісійної електронної мікроскопії (ТЕМ), електронографії, КР- та ЕПР-спектроскопії. Методами електронографії і КР-спектроскопії виявлено кубічну кристалічну структуру CeO_2. ЕПР-спектроскопія показала, що два парамагнітних сигнали мають відношення до ВНТ, а третій обумовлений парамагнітними дефектами CeO_2.

Декорирование углеродных нанотрубок оксидом церия (IV)

**С.Я. Бричка, И.Б. Янчук,
А.А. Кончиц, С.П. Колесник, А.В. Ефанов,
А.В. Бричка, Н.Т. Картель**

*Институт химии поверхности им. А.А. Чуйко Национальной академии наук Украины
ул. Генерала Наумова 17, Киев 03164, Украина
Институт физики полупроводников им. В.Е. Лашкарева Национальной академии наук Украины
пр. Науки 41, Киев 03028, Украина, yanchuk@isp.kiev.ua*

Наночастицы оксида церия (IV) размером 6-10 нм получены на углеродных нанотрубках (УНТ) в результате химической реакции между $Ce(NO_3)_3$ и $NaOH$. Установлены эффективные параметры синтеза наночастиц оксида церия. Нанокомпозиты $УНТ/CeO_2$ охарактеризованы с помощью трансмиссионной электронной микроскопии (ТЭМ), электронографии, КР- и ЭПР-спектроскопии. Методами электронографии и КР-спектроскопии установлена кубическая кристаллическая структура CeO_2. ЭПР-спектроскопия показала, что два парамагнитных сигнала имеют отношение к УНТ, а третий обусловлен парамагнитными дефектами CeO_2.